

Article

Extreme Runoff Estimation for Ungauged Watersheds Using a New Multisite Multivariate Stochastic Model MASVC

Joel Hernández-Bedolla, Liliana García-Romero, Chrystopher Daly Franco-Navarro, Sonia Tatiana Sánchez-Quispe * and Constantino Domínguez-Sánchez *

Faculty of Civil Engineering, Universidad Michoacana de San Nicolás de Hidalgo, Morelia 58030, Mexico; joel.hernandez@umich.mx (J.H.-B.); liliana.romero@umich.mx (L.G.-R.); 1229798x@umich.mx (C.D.F.-N.)

* Correspondence: quispe@umich.mx (S.T.S.-Q.); dsanchez@umich.mx (C.D.-S.); Tel.: +52-443-246-6616 (S.T.S.-Q.)

Abstract: Precipitation is influential in determining runoff at different scales of analysis, whether in minutes, hours, or days. This paper proposes the use of a multisite multivariate model of precipitation at a daily scale. Stochastic models allow the generation of maximum precipitation and its association with different return periods. The modeling is carried out in three phases. The first is the estimation of precipitation occurrence by using a two-state multivariate Markov model to calculate the non-rainfall periods. Once the rainfall periods of various storms have been identified, the amount of precipitation is estimated through a process of normalization, standardization of the series, acquisition of multivariate parameters, and generation of synthetic series. In comparison, the analysis applies probability density functions that require fewer data and, consequently, represent greater certainty. The maximum values of surface runoff show consistency for different observed return periods, therefore, a more reliable estimation of maximum surface runoff. Our approach enhances the use of stochastic models for generating synthetic series that preserve spatial and temporal variability at daily, monthly, annual, and extreme values. Moreover, the number of parameters reduces in comparison to other stochastic weather generators.

Keywords: multivariate stochastic model; extreme rainfall; rainfall-runoff; SCS-CN; probability density functions



Citation: Hernández-Bedolla, J.; García-Romero, L.; Franco-Navarro, C.D.; Sánchez-Quispe, S.T.; Domínguez-Sánchez, C. Extreme Runoff Estimation for Ungauged Watersheds Using a New Multisite Multivariate Stochastic Model MASVC. *Water* **2023**, *15*, 2994. <https://doi.org/10.3390/w15162994>

Academic Editors: Wei Zhang, Nancy A. Barth, Hamid Karimi and Paul Kucera

Received: 29 May 2023

Revised: 31 July 2023

Accepted: 8 August 2023

Published: 19 August 2023



Copyright: © 2023 by the authors. Licensee MDPI, Basel, Switzerland. This article is an open access article distributed under the terms and conditions of the Creative Commons Attribution (CC BY) license (<https://creativecommons.org/licenses/by/4.0/>).

1. Introduction

The frequency analysis of extreme hydrological events to estimate the probability of occurrence is required to design control and management systems [1]. Extreme hydrological events have negative economic and social impacts on human populations. Protection of these populations requires an optimal design of hydraulic structures in terms of a hypothetical extreme event known as design flow or precipitation associated with a particular return period [2].

Often, the return period associated with the design event of a hydraulic structure exceeds the observation periods, and extrapolations must be assumed from the recorded values. Frequency analysis, which relates the magnitude of extreme events to the probability of occurrence using probability distribution functions, is often used to estimate this event [3–5].

A relevant problem in frequency analysis is the selection of the appropriate probability distribution to describe the behavior of the observed data. There are several probability distribution functions for frequency analysis, but none is universally accepted as the best for analyzing hydro-climatological variables [6–8]. Some of the most used distributions in hydrology are normal, log-normal, Gumbel, Weibull, General Extreme Value (GEV), Pearson, and log-Pearson type III [6–9]. In Mexico and Latin America, the Gumbel distribution function has been widely applied as a distribution for evaluating extreme events [10–12].

The estimated values using probability distributions differ from each other. Therefore, it is necessary to select which best fits the time series under analysis. Such a selection

is generally based on goodness-of-fit tests which represent the agreement between the empirical distribution of frequencies and theoretical distribution [13].

Traditionally, these studies to estimate maximum flows have been carried out based on the design storm. However, it is known that this approach is uncertain since peak discharges and hydrographs are strongly dependent on the initial conditions of the basin and on the spatiotemporal distribution of the precipitation [14].

Recently, stochastic weather generators have been proposed to produce synthetic rainfall series [1]. The most common stochastic model is the first-order Markov model with two states, introduced by Gabriel and Newman [15]. The stochastic weather generator MASVC [16] is a multisite multivariate stochastic model, which reproduces the main statistics using normalization and standardization. The multisite standardized series are calibrated by multivariate autoregressive parameters of the stochastic model [17]. Other stochastic generators include: Weather GENERator (WGEN) [18], CLIMA [19], CLIMate GENERator CLIMGEN [20], Long Ashton Research Station-Weather Generator (LARS-WG) [21], École de Technologie Supérieure Weather Generator (WeaGETS) [22], Multi-site Rainfall Simulator (MRS) [23], CLIMate GENERator (CLIGEN) [24], among others.

The objective of applying the multisite multivariate model is to analyze the surface runoff for different return periods [25]. The traditional process for estimating runoff for ungauged watersheds is by using annual maximum rainfall. Subsequently, the best-fit distribution functions are identified, as well as the temporal disaggregation of precipitation. Finally, the maximum runoff is obtained. The present research focuses on acquiring various runoffs through a multisite multivariate stochastic model. The purpose is to use daily scale information and generate synthetic series that allow obtaining return periods associated with the results of the stochastic model. In addition, the SCS-CN method determines the runoffs and the runoff number for the study zones.

2. Materials and Methods

This paper proposes a continuous multisite multivariate model of daily precipitation. Stochastic models allow the generation of maximum precipitation and its association to different return periods. The modeling is carried out in three phases. The first is the estimation of precipitation occurrence by using a two-state multivariate Markov model to calculate the non-rainfall periods. Once the rainfall periods of several storms have been identified, the precipitation amounts are estimated through a process of normalization, standardization of the series, acquisition of multivariate parameters, and generation of synthetic series [16]. The maximum values show consistency for different return periods, therefore, a more reliable estimation of the maximum discharge [25].

2.1. Multisite Multivariate Stochastic Model MASVC

Stochastic modeling of precipitation has been investigated mainly at a daily scale, which can be simulated by a short memory model for both past and future cases [26], and is used for runoff determination [27]. Precipitation data are necessary to determine short-term hydrological variability [28], while temporal analysis of minutes to hours is commonly applied [29,30]. On a daily scale, stochastic models have been developed for rainfall analysis [31,32].

In essence, the stochastic modeling of different scales represents a general problem-solving process. However, each stochastic model has its particularities, which will depend on the analysis scale [33]. The general objective of the current investigation is to use the multisite multivariate stochastic model MASVC [16]. This model simulates rainfall with daily time dependence and analyzes rainfall in two phases, divided into occurrence and amount. MASVC estimates rainfall occurrence, and the amount of rainfall model is a first-order continuous autoregressive model, although it has been used to generate rainfall and temperatures [16].

The purpose of utilizing the MASVC 1.0 software is to generate 1000 series of equal lengths to obtain different return periods. Although it is common for stochastic models to

present uncertainty in the extreme quartile [10], in this case, the stochastic model is consistent with daily maximum precipitation data. Figure 1 displays the proposed methodology.

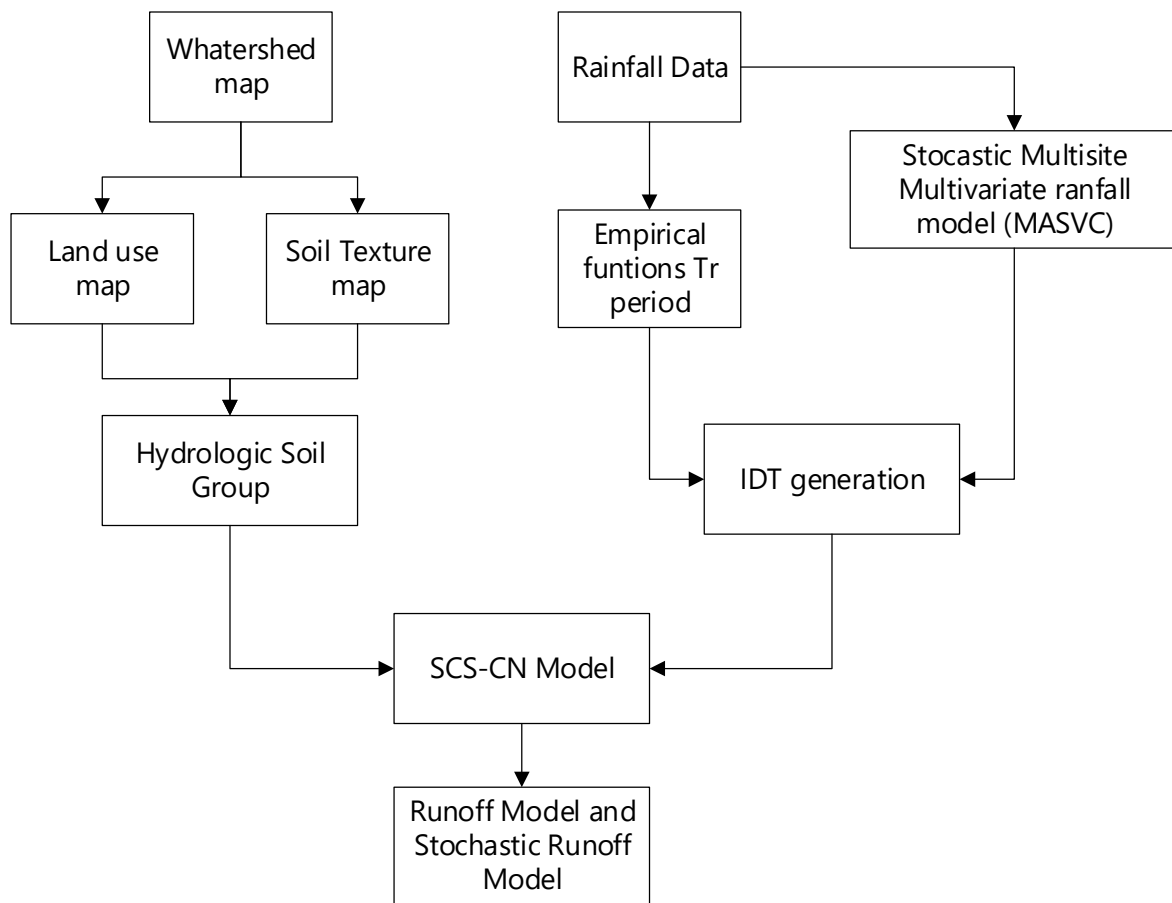


Figure 1. Proposed methodology.

MASVC applies a Wilks approach for the occurrence process [34] based on conditional and critical normal probabilities, which depend on the previous day. The multivariate occurrence process uses a spatially correlated normal matrix. A wet day is the normal vector for a day greater than a critical probability. This transition matrix varies daily.

MASVC uses the random spatially correlated normal matrix $n = [M]'[N]$ to produce synthetic occurrence series. M' is the lower triangular matrix, and N is the random normal matrix. This matrix was used to generate multivariate precipitation occurrences.

The multivariate autoregressive coefficient's matrix was calibrated for rainfall generation, resulting in the residual series $(\varepsilon_\tau = [\phi]_0^{-1}(\{z\}_\tau - [\phi]_1\{z\}_{\tau-1}))$. Where ε_τ is the residual series, $[\phi]_0^{-1}$ is the inverse lag-0 autoregressive coefficient matrix, $[\phi]_1$ is the lag-1 autoregressive coefficient matrix, $\{z\}_\tau$ is the standardized vectors for day τ , and $\{z\}_{\tau-1}$ is the standardized vectors for the previous day $\tau - 1$. All the units for the vectors and matrices are non-dimensional. The residual series satisfied the mean, correlation, standard deviation, and skewness coefficient of the entire series within the confidence limits according to 95% of normal distribution [35–37]. Next, a random number with a normal distribution (ε) obtains the standardized series (z_t) and inverse normalization (y_τ^{-1}).

2.2. Probability Density Functions (PDF)

Traditional methods to obtain extrapolations for a return period use distribution functions. However, they have a disadvantage in that they apply few precipitation records [38]; one per year. Therefore, they have higher uncertainty [1,39], and fitting PDFs' distribution

suffers from numerical stability [40]. The most common distribution functions are normal, log-normal, gamma, log-Pearson type III, Gumbel, and log-Gumbel [2,38,41–46].

Normal PDF. The expression that determines a normal distribution is given as follows by Equation (1):

$$F(x) = \frac{1}{\sigma_y \sqrt{2\pi}} e^{-\frac{1}{2} \left(\frac{x-\mu_y}{\sigma_y}\right)^2} \tag{1}$$

where μ_y is the location parameter and σ_y is the scale parameter.

2-Parameter Log-Normal PDF. The mathematical expression that determines this function is given by Equation (2):

$$F(x) = \int_0^x \frac{1}{x\sigma_y \sqrt{2\pi}} e^{-\frac{1}{2} \left(\frac{\ln x - \mu_y}{\sigma_y}\right)^2} dx \tag{2}$$

where μ_y is the location parameter and σ_y is the scale parameter.

3-Parameter Log-Normal PDF. The mathematical expression corresponding to this distribution is Equation (3):

$$F(x) = \int_0^x \frac{1}{(x-x_0)\sigma_y \sqrt{2\pi}} e^{-\frac{1}{2} \left(\frac{\ln(x-x_0) - \mu_y}{\sigma_y}\right)^2} dx \tag{3}$$

where x_0 is the location parameter, μ_y is the scale parameter, and σ_y is the shape parameter.

2-Parameter Gamma PDF. The 2-parameter gamma function is given by Equation (4):

$$F(x) = \int_0^x \frac{x^{\beta-1} e^{-\frac{x}{\alpha}}}{\alpha^\beta \Gamma(\beta)} dx \tag{4}$$

where α is the scale parameter, β is the shape parameter, and $\Gamma(\beta)$ is the complete gamma function.

3-Parameter Gamma PDF. For the 3-parameter gamma function (also known as Pearson) Equation (5) is considered:

$$F(x) = \int_0^x \frac{1}{\alpha \Gamma(\beta)} \left(\frac{x-x_0}{\alpha}\right)^{\beta-1} e^{-\left(\frac{x-x_0}{\alpha}\right)} dx \tag{5}$$

where α is the scale parameter, β is the shape parameter, $\Gamma(\beta)$ is the gamma function, and x_0 is the location parameter.

Log-Pearson III PDF. For this PDF the same expression that describes the 3-parameter gamma function is used except that the base-10 logarithmic transformation of the series is performed.

Gumbel PDF. This model is defined by Equation (6):

$$F(x) = \exp - \left[\exp \left(- \left[\frac{x-\mu}{\alpha} \right] \right) \right] \tag{6}$$

where μ is the location parameter and α is the scale parameter.

Log Gumbel PDF. The PDF log-Gumbel is defined by Equation (7):

$$F(x) = \frac{1}{\alpha x} \exp \left\{ - \exp \left[- \frac{\ln(x) - \mu}{\alpha} \right] - \frac{\ln(x) - \mu}{\alpha} \right\} \tag{7}$$

where μ is the location parameter and α is the scale parameter.

For the PDF performance, the HidroEsta 2.0 software was used through the Kolmogorov–Smirnov test, which compares the maximum absolute value of the difference between the observed and the estimated probability density function [47–50].

$$D = \max |F_O(x_m) - F(x_m)|$$

This value is compared with the significance level, so it needs to be less than the latter to accept the null hypothesis.

2.3. Curves IDT

The curves' intensity–duration–return period (IDT) was elaborated based on the results of the stochastic multisite multivariate model and the PDFs. The hyetograms of construction design were carried out using the method proposed by Kuichling [51]. This method consists of the maximum daily precipitation associated with various return periods. It associates the maximum intensity curves for different durations in which values such as intensity (I_d), maximum precipitation (P_d), and a constant to determine the duration of a known rainfall (K) are estimated. The expressions that define the model are the Equations (8)–(10):

$$I_d = \frac{K}{(1-e)d^e} \quad (8)$$

$$P_d = \frac{Kd^{1-e}}{1-e} \quad (9)$$

$$K = \frac{P(1-e)}{24^{1-e}} \quad (10)$$

where I_d is the intensity associated with a specific duration, P_d is the precipitation associated with a specific duration, K is the parameter associated with concentration time and maximum rainfall, e is the coefficient defined as a function of concentration time, and d is the interval of hours as a function of concentration time.

The Kirpich method can be applied in IDT analysis to estimate the rainfall intensity for a given duration and return period. The Kirpich method estimates the concentration time (T_c), which is the time it takes for the entire contributing area to generate runoff to a specific point. In this study, T_c is considered equal to the rainfall duration. Furthermore, it is an essential parameter in hydrological calculations to determine peak flow rates, design stormwater management systems, and analyze flood potential.

2.4. Soil Conservation Service Curve Number Method (SCS-CN)

The Soil Conservation Service Curve Number (SCS-CN) method is applied to estimate runoff from small-to-medium-sized watersheds. The SCS-CN method was established in 1954 by the USDA SCS and since then has been widely used [52–59] in GIS [60] for tropical catchment [61]. This method is presented in Equations (11)–(14):

$$P_e = \frac{(P - I_a)^2}{(P - I_a) + S} \quad (11)$$

where P_e is the accumulated precipitation excess, P is the accumulated rainfall, and S is the potential maximum retention. From the experimental catchments analysis of results, the SCS developed an empirical relation between I_a and S . This relation is the following Equation (12):

$$I_a = 0.2S \quad (12)$$

Therefore, the cumulative excess is considered as Equation (13):

$$P_e = \frac{(P - 0.2S)^2}{(P - 0.8S)} \quad (13)$$

The S is the potential maximum retention and is given by Equation (14):

$$S = \frac{25400 - 254CN}{CN} \quad (14)$$

where *CN* is the curve number, which varies from 25 for permeable soils with high infiltration to 100 for bodies of water.

2.5. Case Study

The Rio Grande de Morelia watershed is located in the north-central portion of the state of Michoacan in Mexico. The area belongs to the endorheic basin of Lake Cuitzeo in the Lerma-Santiago Hydrological Administrative Region 12 (Figure 2). The basin has an approximate area of 1565 km². The region’s predominant climate is subhumid, with an average annual rainfall of 815 mm. The main stream of the Rio Grande de Morelia and its main tributaries (1 Itzicuaros, 2 Alberca, 4 Barajas, 5 Arroyo de Tierras, 6 Rio Chiquito, 8 Atapaneo, 12 Quinceo, 13 Mora Tovar, 14 Calabocito, 15 Calabozo, and 16 Carlos Salazar) will be considered for the subbasins. The weather stations were obtained from the national meteorological service belonging to the National Water Commission (CONAGUA), which are available at <https://smn.conagua.gob.mx> (accessed on 20 January 2023). Four weather stations with influence in the study area were identified: 16022, 16247, 16055, and 16081. The available data for these stations are from 1980 to 2009 (Table 1).

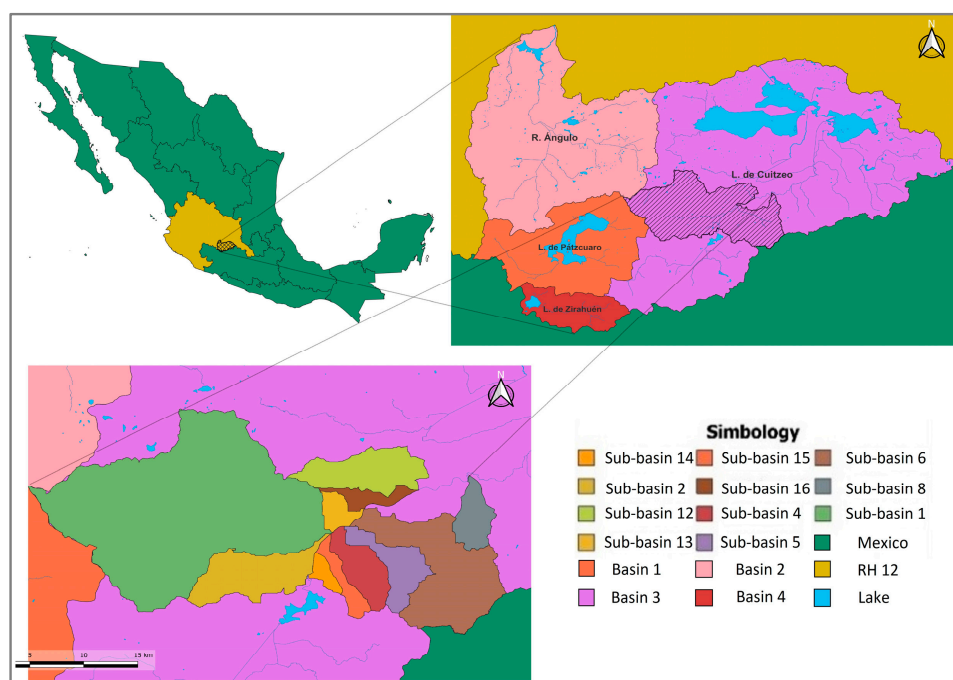


Figure 2. Location of the subbasins in Morelia. 1 Itzicuaros, 2 Alberca, 4 Barajas, 5 Arroyo de Tierras, 6 Rio Chiquito, 8 Atapaneo, 12 Quinceo, 13 Mora Tovar, 14 Calabocito, 15 Calabozo, and 16 Carlos Salazar. Patzcuaro basin 1, Angulo basin 2, Cuitzeo basin 3, Zirahuén basin, Hydrologic Región 12.

Table 1. Stations considered in this study.

Station	Latitude (°)	Longitude (°)	Elevation (msnm)	Years	Total Annual Precipitation (mm/year)	Pmax * (mm/year)
16022	19.625	−101.281	2096	1980–2009	811.8	78
16247	19.675	101.392	2097	1980–2009	700.7	75.3
16055	19.652	−101.151	2180	1980–2009	1092.25	97
16081	16.289	−101.176	1913	1980–2009	772.21	80.1

Note: * Maximum precipitation per year.

3. Results

To estimate the main statistics for the case study, first, a minimum wet threshold was assumed which can be the reading of the climate stations (0.1 mm). This limit was considered for the wet and dry days. The maximum 24 h rainfall for the Rio Grande of Morelia basin is between 21 and 97 mm. The average annual precipitation is between 700.7 and 1092.25 mm for the various subbasins. The number of days with precipitation occurrence is between 95 and 127 days per year with rainfall. The maximum 24 h precipitation for the four stations is between 11 and 97 mm, while the average annual precipitation is between 700 and 1090 mm for the different subbasins.

3.1. Multisite Multivariate Stochastic Results

The transition probabilities for all stations are shown in Figure 3. This probability indicates that the occurrence process is most likely on a wet day between 0.5 and 0.68. On the other hand, for a wet day following a dry day, the probability decreases to 0.1 to 0.12. The results indicate two consecutive wet days in wet seasonality are most common (June to October). The dry seasonality is between November to May.

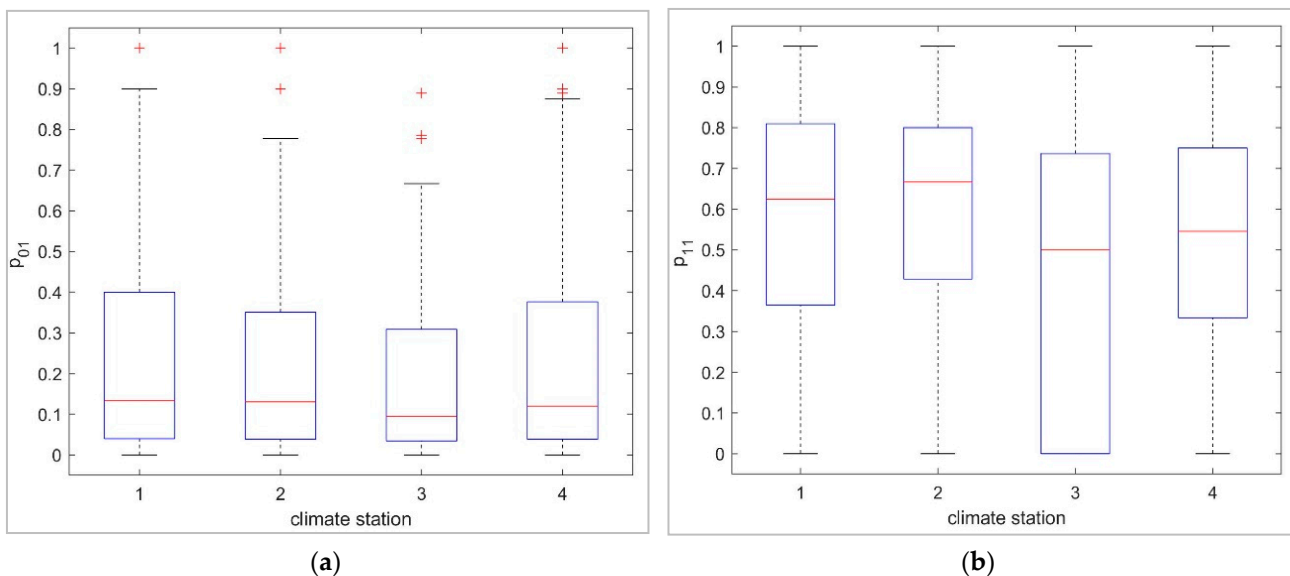


Figure 3. Transition probabilities for all stations (a) p_{01} and (b) p_{11} , (+) extreme data points considered outliers.

Wet days series are known to skew to the right. To remove the skew, a log-gamma normalization was applied and the confidence limits of 95% were verified (Figure 4). The daily skewness coefficient of the historical rainfall is between 0.55 to 1.02 for all stations. After normalization, the skewness coefficient was ± 0.059 . These results can be considered the log-gamma transformation, which removes the skew of historical rainfall.

Standardization was performed using the normalized mean and standard deviation. MASVC uses the Fourier series to reduce the number of parameters. After standardization, multisite multivariate autoregressive coefficients were calculated by Cholesky decomposition to generate synthetic series.

The main statistics of the residual series were calculated. The mean, standard deviation, skewness coefficient, and lag-one autocorrelation are presented in Table 2. Moreover, the normal function was calculated and the results of the residual series were evaluated (Figure 5). The residual series has a mean near zero, the maximum standard deviation error is 0.0895, the skewness coefficient is between -0.1212 and 0.5622 , and the lag-one autocorrelation is around -0.0581 and 0.0461 . The mean, standard deviation, and lag-one autocorrelation are within the confidence limit of 95%. The skewness coefficient is within the confidence limit of 99%.

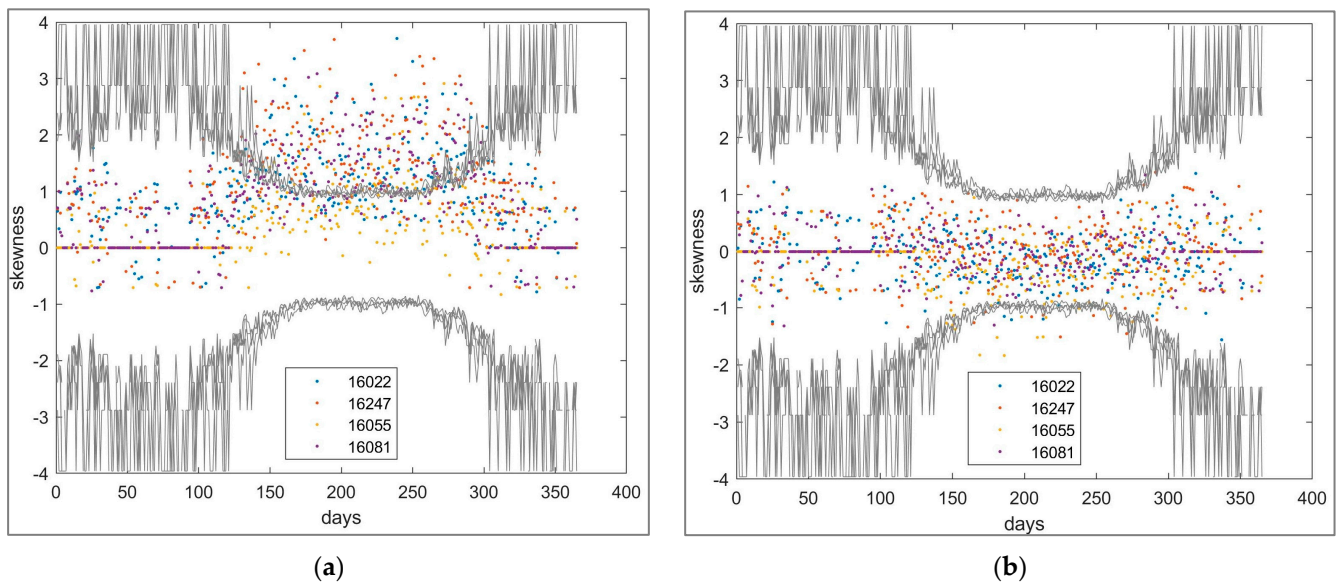


Figure 4. Daily average of skewness coefficient (1980–2009) with confidence Anderson limits: (a) historic rainfall and (b) normalized rainfall.

Table 2. Normality analysis for residual series for both M1 and M2 (wet threshold 0.001).

Statistical/Station	16055	16081	16022	16247
Mean	−0.0084	−0.0035	0.080	−0.078
Standard deviation	1.0431	1.0843	1.3315	1.0895
Skewness coefficient	−0.1212	0.3246	0.5622	−0.0939
Lag-one autocorrelation	0.0239	0.0420	0.0461	−0.0581
AIC	−2145	−1995	−4733	−2652

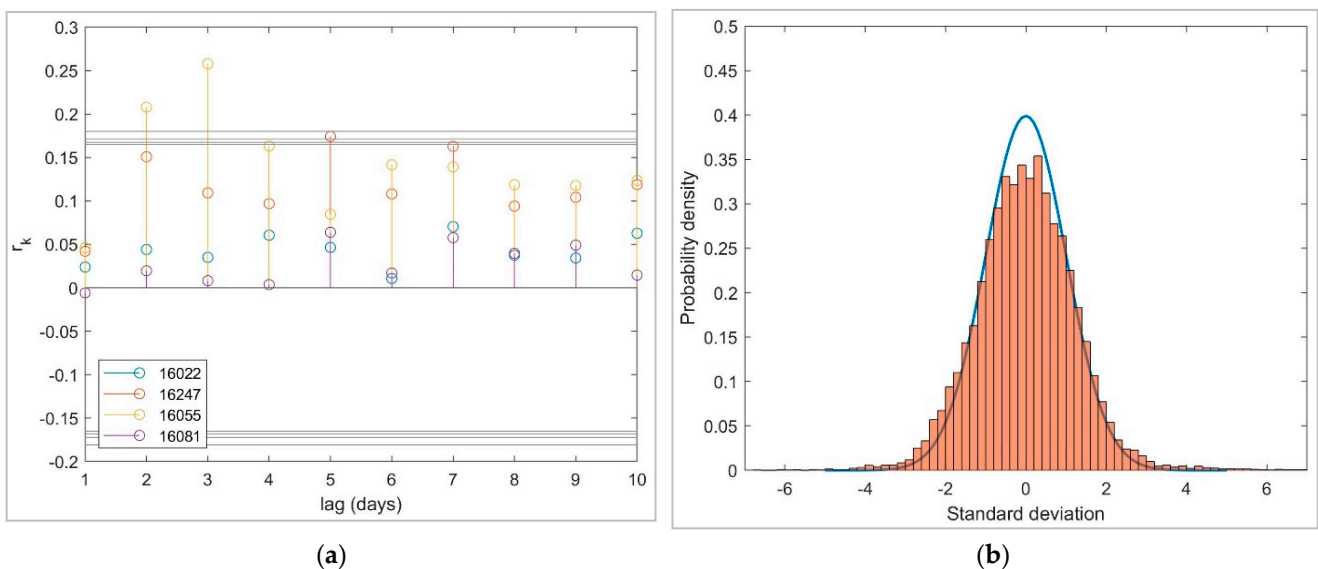


Figure 5. Residual series for all subbasins: (a) autocorrelation lag–10 and (b) normal standard distribution (blue) and residual (bars).

Finally, the synthetic series were generated. A total of 1000 synthetic series were made considering the same length as the sample (30 years). The statistical sum and mean were estimated for both synthetic and historical series. The sum of the number of rainy days

in 30 years was calculated for the historical series. The results offer a good correlation between the observed and simulated values.

The occurrence of multisite multivariate synthetic series for the four weather stations were obtained. Figure 6 represents the sum of wet days in 30 years. For the simulated series, the mean of the sum of wet days were calculated. Afterward, the K–S test was performed to verify that the results came from the same distribution considering 95% confidence. For all analyzed stations, daily occurrences vary from the 1:1 line ± 5 days (Figure 6). The variation of precipitation occurrence with regard to the number of rainy days presents a variability due to the number of parameters used in the transition matrices p_{01} and p_{11} (4).

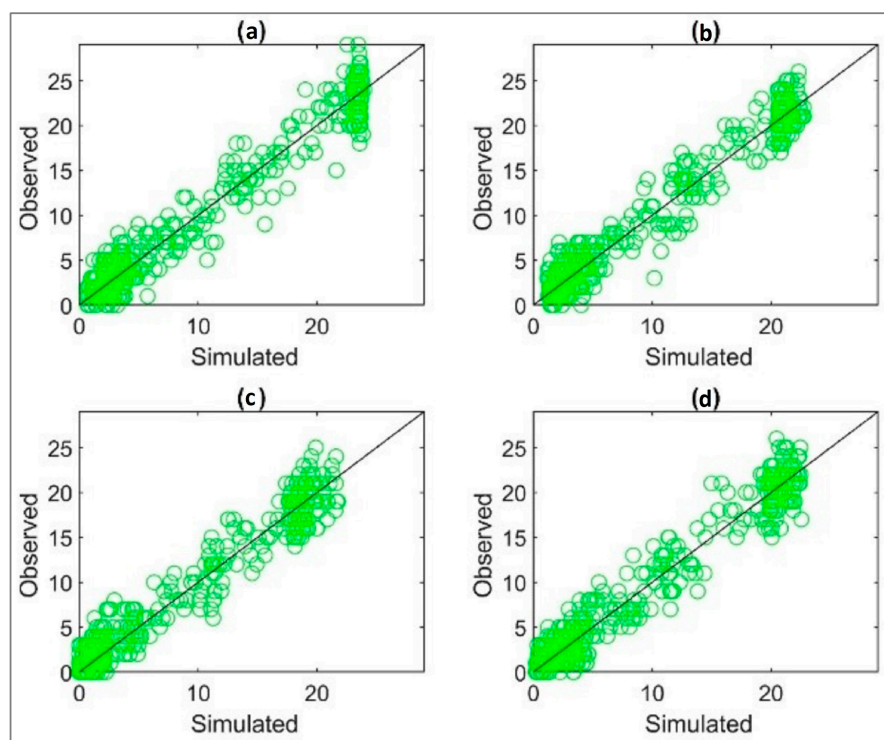


Figure 6. Scatter plots for rainfall occurrence (mean of 30 observed years and 1000 simulated series) for the four stations: (a) 16022, (b) 16247, (c) 16055, and (d) 16081.

The precipitation for the four stations was generated by the log-gamma transformation, which produced the best results (Figure 7). For the daily precipitation amount (without zeros), the mean and standard deviation of 1000 synthetic series were calculated. The observed precipitation is in the range of confidence limits at 95%.

The multisite multivariate stochastic model for mean daily precipitation has a deviation of ± 10 mm. The observed and generated series are not significantly different according to the K–S test, which indicates that they came from the same distribution. In addition, they have the same average according to the t -test and the same median according to the Wilcoxon test.

The maximum precipitation of each year was extracted from 30 data and assigned with their respective return period to obtain the maximum historical series. In the case of the generated synthetic series, the maximum of each year was extracted for 1000 series, and the average was obtained as being equal to 30 years. The results of the multisite multivariate stochastic model are shown in Figure 8. The different graphs were constructed for the four stations: 16022, 16247, 16055, and 16081. The results indicate that for station 16022, there are underestimates for a Tr less than 8 years (10 mm), and for the rest of the period, there is an adequate adjustment. For station 16247, there is a suitable adjustment for return periods between 1 and 15. Subsequently, it tends to overestimate the maximum precipitation by 11 mm. Station 16055 presents an acceptable trend for the different return

periods but nevertheless overestimates return periods between 10 and 20. Station 16081 displays underestimates for return periods less than 10 and presents a proper adjustment for return periods up to 30.

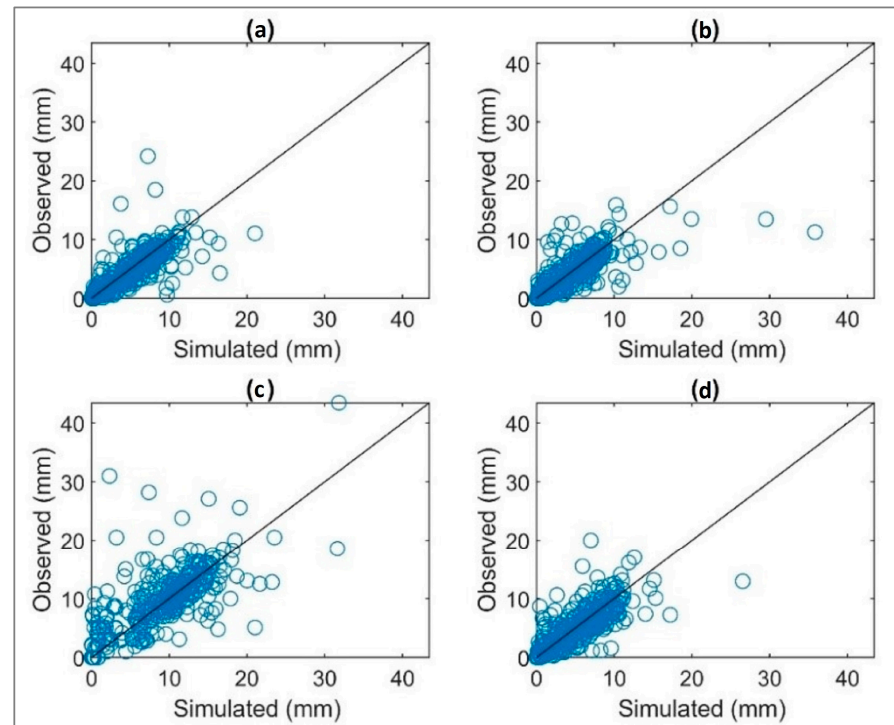


Figure 7. Scatter plots for observed mean versus daily simulated rainfall (mean of 30 observed years and 1000 simulated series) for stations: (a) 16022, (b) 16247, (c) 16055, and (d) 16081.

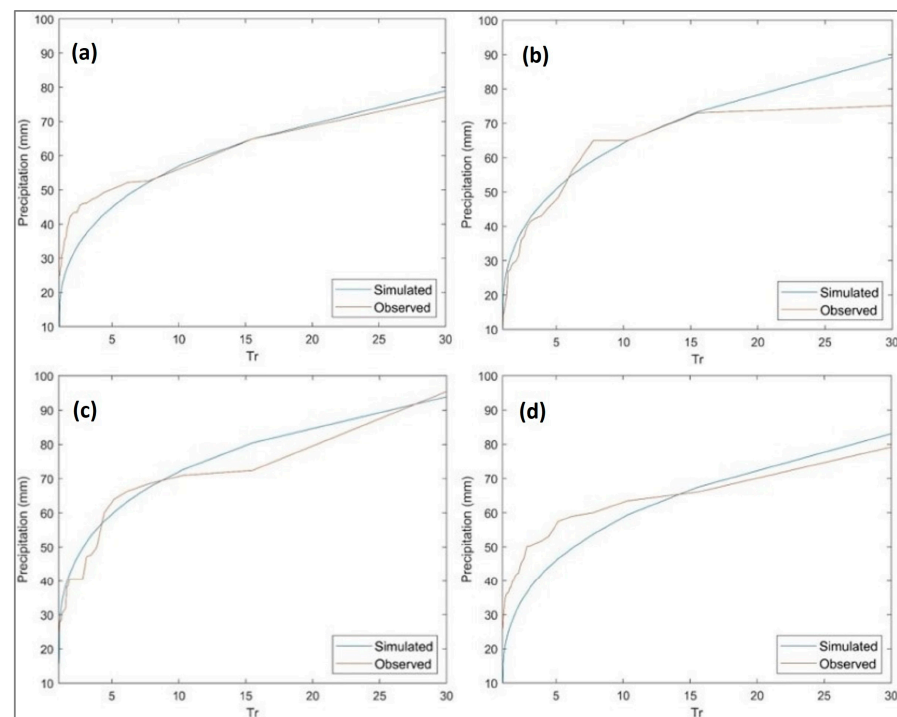


Figure 8. Observed and simulated maximum daily rainfall for 30 years (mean of 30 observed years and 1000 simulated series) for the four stations: (a) 16022, (b) 16247, (c) 16055, and (d) 16081.

3.2. PDFs

Different distribution functions evaluated for the maximum annual rainfall were estimated using the Smirnov–Kolmogorov test for each of the PDFs. These results indicated that for station 16055, the best fitting function was log-Gumbel $p = 0.0871$. For station 16081, the most acceptable was Gumbel $p = 0.045$. For station 16022, it was log-normal of 3 parameters ($p = 0.0696$), and for station 16247, log-normal of 2 parameters. The results for the different stations are presented in Table 3. The basin is affected by extreme rainfall events such as heavy rainfall, storms, and tropical cyclones. These events often exhibit high variability in their occurrence and intensity, leading to localized flooding, landslides, and other hydrological hazards (Appendix A). This is the main reason why different distribution functions are adjusted (Table 4).

Table 3. Smirnov–Kolmogorov test for each of the PDFs fitted to the maximum 24 h precipitation series for each station.

Function/Station	16055	16081	16022	16247
Normal	0.1977	0.1138	0.1932	0.1193
Log-Normal 3P	0.1064	0.0592	0.0696 *	0.1044
Log-Normal 2P	0.1187	0.0618	0.1164	0.0907 *
Gamma 2P	0.1427	0.0798	0.1433	0.1025
Gamma 3P	N/A	0.05595	N/A	0.09575
Log Pearson III	0.09761	0.0511	N/A	N/A
Gumbel	0.1347	0.045 *	0.1478	0.0994
Log Gumbel	0.0871 *	0.0596	0.079	0.0924

Note: * Best fit.

Table 4. Comparison of MASVC versus PDFs for all stations.

Model	TR	16022	16247	16055	16081
MASVC	2	34.99	40.05	47.73	31.65
	5	43.78	50.47	59.49	47.45
	10	58.26	64.33	71.87	59.36
	20	69.58	79.31	84.41	72.07
	50	87.33	99.25	101.34	91.33
	100	102.25	112.2	116.51	105.23
PDF	2	40.66	41.01	31.27	42.7
	5	52.61	56.2	43.61	53.75
	10	61.63	66.27	54.35	61.07
	20	71.03	75.93	67.13	68.09
	50	84.27	88.49	88.23	77.18
	100	95.02	98	108.28	83.99

3.3. SCS-CN

The contribution subbasins of each of the streams under study were delimited by applying ArcGIS 10.5. For this purpose, a digital elevation model (DEM) that covers the entire study area was used. In this process, the DEM provided by INEGI, with a resolution of 15 m extracted from the Mexican Elevation Continuum, was utilized as input. Once the DEM was obtained and the exit points of each subwatershed were defined using geographic information systems (GIS), the subbasins were delineated (Figure 9). Afterward, their geomorphological characteristics were determined, as well as the area (km²), height difference (m), length of the main channel (m), slope (%), and concentration time (h).

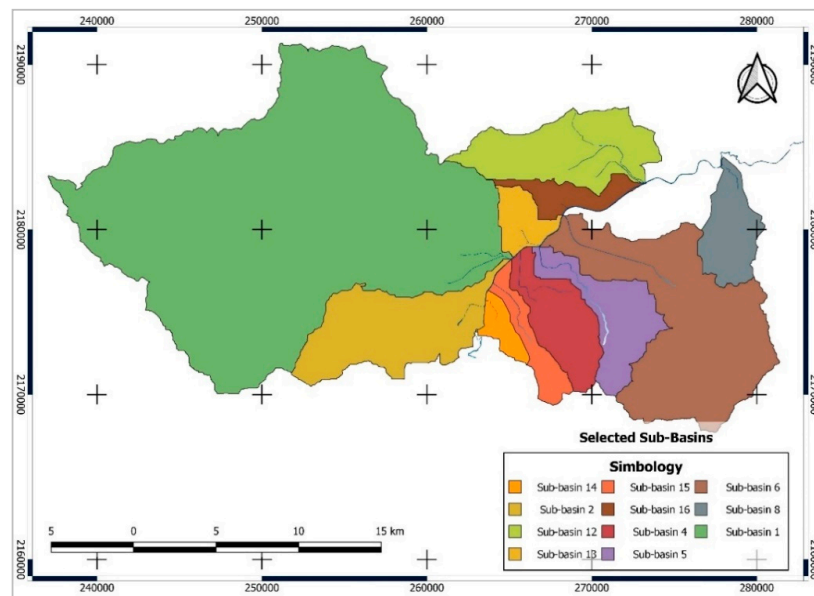


Figure 9. Urban subbasins in Morelia. 1 Itzcuaros, 2 Alberca, 4 Barajas, 5 Arroyo de Tierras, 6 Rio Chiquito, 8 Atapaneo, 12 Quinceo, 13 Mora Tovar, 14 Calabocito, 15 Calabozo, and 16 Carlos Salazar.

To determine the runoff number, information from the INEGI Soil Use and Vegetation chart scale 1:250,000 (E14-1) was used to identify the different land uses. In addition, the Edaphological chart scale 1:250,000 (E14-1) was applied, from which different soil textures were extracted. Using ArcGIS 10.5, the maps were reclassified, and runoff numbers were assigned. For the watershed study, there are curve number (CN) values between 44 and 87. The lowest values are located in infiltration zones, very permeable soils, and thick forests. The high CN values are found in the urban area of Morelia, where the soil characteristics are fine with little infiltration capacity. The mean CN for all subbasins is 83.03, which indicates an urban basin. Figure 10 shows all the reclassifications for the subbasin under study, and Table 5 shows the values for each subbasin. Urban subwatersheds tend to have CN values greater than 80, contrary to headwater micro-watersheds which include larger non-urbanized areas and greater infiltration capacity due to soil and vegetation.

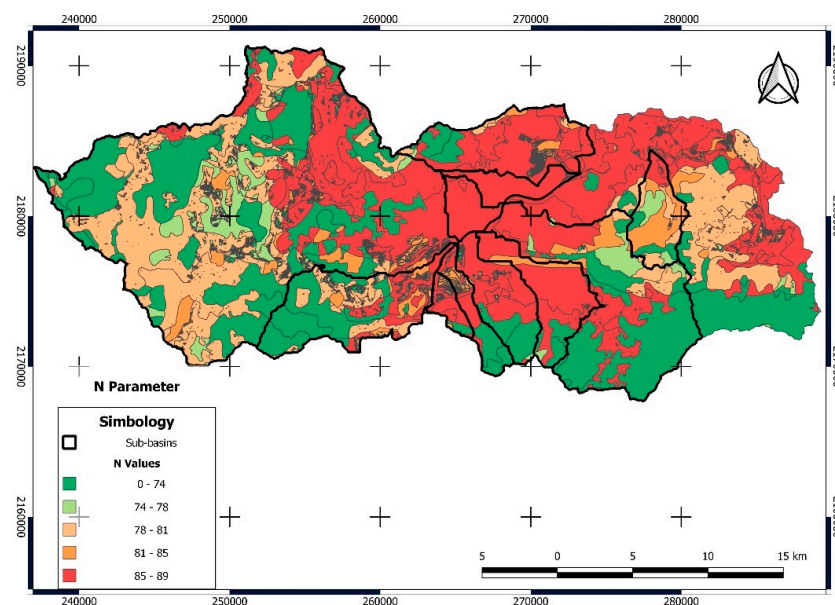


Figure 10. Curve number for all subbasins.

Table 5. Geomorphological characteristics and curve number of the subbasins study.

Subbasin *	Area (km ²)	Height Difference (m)	Length of the Main Channel (m)	Slope (%)	Concentration Time (h)	CN
1	308.32	898	30,833.01	2.41	3.62	76.35
2	47.62	1132	16,106.46	5.72	1.56	78.36
4	24.3	459	11,451.81	5.32	1.49	84.47
5	26.67	561	12,862.88	4.58	1.58	83.14
6	86.79	416	21,086.86	1.13	3.13	77.03
8	18.85	230	9394.3	2.46	1.55	84.16
12	40.19	792	14,307.83	4.77	1.56	85.09
13	10.01	258	4614.52	5.14	0.65	86.87
14	6.11	220	4114.46	3.95	0.61	86.02
15	11.3	671	9878.71	3.67	1.08	84.67
16	10.71	1.93	453.54	0.43	0.29	87.21

Note: * 1 Itzicuaros, 2 Alberca, 4 Barajas, 5 Arroyo de Tierras, 6 Rio Chiquito, 8 Atapaneo, 12 Quinceo, 13 Mora Tovar, 14 Calabocito, 15 Calabozo, and 16 Carlos Salazar.

Once the model parameters were obtained, the design hyetograms corresponding to the analyzed periods for each subbasin were estimated with MASVC 1.0 software and Hydroesta 2.0 software. Finally, the surface runoff was calculated.

3.4. Determination of Surface Runoff for All Subbasins

After the design hyetograms were obtained, hydrographs were calculated using the curve model formulated by the U.S. Soil Conservation Service (SCS-CN), which determines runoff thresholds as a function of runoff curve number. Table 6 displays different return periods and the maximum surface runoff for each subbasin. The main results indicate the surface runoff is lower for return periods 2, 5, and 10 for MASVC-SCS-CN. For return periods of 20 to 100, the MASVC-SCS-CN surface runoff is higher than PDF-SCS-CN, a consequence of the subestimation of 24 h precipitation for return periods less than 20.

Table 6. Surface runoff for all subbasins MASVC-SCS-CN and PDF-SCS-CN.

Model	* Subbasin/Tr	2	5	10	20	50	100	
MASVC-SCS-CN	1	9.68	35.01	88.48	166.82	298.97	394.90	
	2	0.32	1.49	9.86	20.72	44.11	68.85	
	4	0.11	1.45	5.39	11.93	25.73	38.10	
	5	1.45	6.11	13.08	22.26	36.62	53.63	
	6	4.38	13.76	28.25	47.08	78.03	110.21	
	8	0.11	1.17	25.30	30.72	38.93	44.85	
	12	0.93	2.51	9.08	19.89	42.50	62.65	
	13	0.05	0.47	2.86	7.39	17.72	27.20	
	14	0.02	0.10	1.75	4.29	10.12	16.44	
	15	0.01	0.12	1.93	4.64	10.78	17.52	
	16	0.23	0.94	2.95	6.09	12.43	17.95	
	PDF-SCS-CN	1	10.56	52.59	104.17	142.81	217.25	280.62
		2	0.98	7.06	16.79	25.42	44.15	62.26
		4	0.91	4.24	5.08	7.64	17.92	23.30
		5	0.33	1.11	5.81	11.47	28.00	48.51
		6	2.21	3.06	13.73	25.48	59.66	101.38
8		0.67	3.16	3.79	5.68	13.39	17.45	
12		1.40	6.67	7.99	12.02	28.33	36.87	
13		0.11	1.73	2.15	3.72	10.53	14.29	
14		0.10	0.90	2.74	4.70	8.98	13.24	
15		0.06	1.34	3.74	6.01	11.05	16.06	
16		0.60	2.29	2.61	3.91	8.65	11.06	

Note: * 1 Itzicuaros, 2 Alberca, 4 Barajas, 5 Arroyo de Tierras, 6 Rio Chiquito, 8 Atapaneo, 12 Quinceo, 13 Mora Tovar, 14 Calabocito, 15 Calabozo, and 16 Carlos Salazar.

4. Discussion

Temporal and spatial variability studies of extreme precipitation are challenging for risk assessment [62]. Probability density functions (PDFs) and stochastic weather generators are two approaches used in hydrology to model and simulate maximum rainfall events. PDFs represent the statistical distribution of maximum rainfall events based on observed data, which does not provide doubtful information [63]. Furthermore, PDFs overestimate precipitation events [64,65]. However, PDFs alone do not provide a temporal sequence of rainfall events, nor do they capture the temporal correlation and patterns of rainfall occurrence [1,62].

Stochastic weather generators reduce the uncertainty of the calculated floods [1]. Moreover, stochastic weather generators reproduce long series of extreme precipitation [66]. MASVC simulates continuous synthetic rainfall sequences based on statistical properties of observed weather data. This generator captures the temporal correlation and patterns of weather variables, as well as rainfall. MASVC uses a combination of statistical parametrization to represent the characteristics of weather variables and their interrelationships. MASVC incorporates multiple statistical parameters, including mean, variances, autocorrelation, and other higher-order moments. By simulating synthetic rainfall sequences, MASVC can generate long-term, time-series rainfall data that captures the statistical properties of historically extreme rainfall events. They are applicable for hydrological modeling, flood forecasting, and water resources management, as they provide realistic representations of rainfall patterns and capture rainfall variability over time [67–69]. MASVC was applied to semiarid and humid regions with good performance [70]. The limitations of MASVC are that it requires 30 years of historic rainfall and does not consider snow in the stochastic model.

The stochastic rainfall generator MASVC can simulate temporal and spatial characteristics of rainfall, capturing the variability and patterns in real-world rainfall data [71–73]. It considers the timing, duration, intensity, and occurrence of rainfall events, allowing for the generation of realistic rainfall sequences that provide the behavior of observed data. In contrast, PDFs offer information about the statistical distribution of rainfall but do not inherently capture temporal and spatial variability [74].

This approach significantly simplifies the process of generating precipitation data, which implies a relevant advantage and versatility concerning other stochastic generators and PDFs. The reduction of parameters is an essential factor addressed in this approach to determine the maximum rainfall amounts, in addition to considering the continuous modeling for all days, months, and years of simulation. Furthermore, the SCS-CN method is widely used for hydrologic studies in an ungauged basin for the National Water Commission (CONAGUA) [75–88].

5. Conclusions

This article presents a multisite multivariate stochastic model for generating daily rainfall consistent to mean and maximum precipitation. MASVC is a two-step model that first produces the multivariate occurrence process. Afterward, a nonzero amount of rainfall is generated using a continuous nonparametric multisite multivariate stochastic autoregressive first-order model. This model can reproduce daily maximum, monthly, and total annual precipitations. The approach is an efficient algorithm for the entire range of precipitation. Moreover, MASVC is a continuous semiparametric model that can reduce the number of parameters compared to other generators and is capable of reproducing maximum and minimum precipitation.

Finally, the surface runoff using the proposed methodology MASVC-SCS-CN is determined and compared with the PDF-SCS-CN. The main difference between the MASVC and PDFs is the scale analysis. MASVC uses the daily series for the entire historical period and generates multiple equiprobable synthetic series that can occur in the study area. The greater the number of synthetic series, the longer the return periods can be extended. On the other hand, PDFs use a limited number of data, only one per year.

This approach significantly improves the process of generating surface runoff with greater occurrence confidence, which implies an overall advantage and versatility concerning PDF-SCS-CN.

Author Contributions: Conceptualization, J.H.-B. and S.T.S.-Q.; methodology, J.H.-B. and L.G.-R.; software, C.D.F.-N. and J.H.-B.; validation, S.T.S.-Q., C.D.-S., and J.H.-B.; formal analysis, C.D.F.-N. and J.H.-B.; investigation, J.H.-B. and L.G.-R.; resources, C.D.-S.; data curation, C.D.F.-N.; writing—original draft preparation, L.G.-R. and J.H.-B.; writing—review and editing, C.D.-S. and S.T.S.-Q.; visualization, L.G.-R.; supervision, S.T.S.-Q.; project administration, C.D.-S.; funding acquisition, C.D.-S. and S.T.S.-Q. All authors have read and agreed to the published version of the manuscript.

Funding: The authors acknowledge the support from the Institute of Science, Technology and Innovation (ICTI) for its financial support through the project “PICIR-069 Sistema de mitigación del riesgo contra inundaciones de la Ciudad de Morelia”.

Data Availability Statement: Not applicable.

Acknowledgments: The authors wish to thank the Universidad Michoacana de San Nicolás de Hidalgo. The second and third authors wish to thank the National Council of Humanities, Science and Technology of Mexico (CONAHCyT) for the financial support of their postgraduate studies. Additionally, the authors acknowledge the support from the Institute of Science, Technology and Innovation (ICTI) for its financial support through the project “PICIR-069”. Finally, we also value the anonymous reviewers and the editor for their constructive comments on the manuscript.

Conflicts of Interest: The authors declare no conflict of interest.

Appendix A

Regional analysis of the maximum precipitation in the Rio Grande Basin are presented in Figure A1. This shows different patterns of maximum rainfall and regional changes for the subbasins. The grid interpolation uses inverse distance weight interpolation (IDW). QQ plot of PDFs is shown in Figures A2–A6.

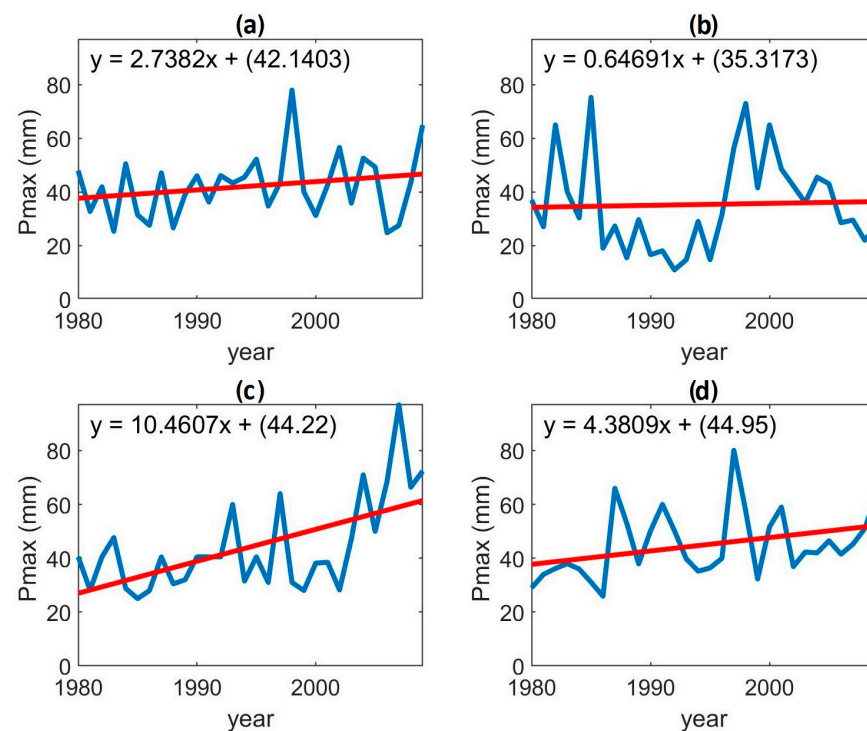


Figure A1. Temporal variation of maximum precipitation for the four stations; (a) 16022, (b) 16247, (c) 16055, and (d) 16081, blue line is the maxima precipitation (1980 to 2009) and red line is the linear regression.

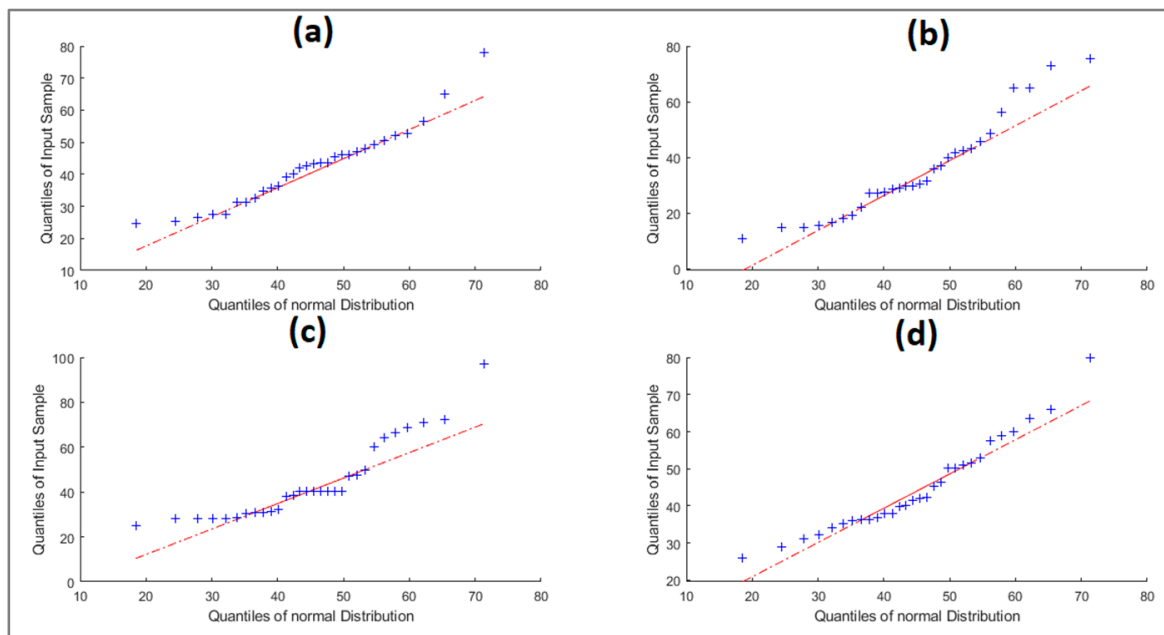


Figure A2. QQ plots normal distribution for the four stations; (a) 16022, (b) 16247, (c) 16055, and (d) 16081. Blue plus signs are the normal adjusted precipitation and dotted lines theoretical normal quantiles.

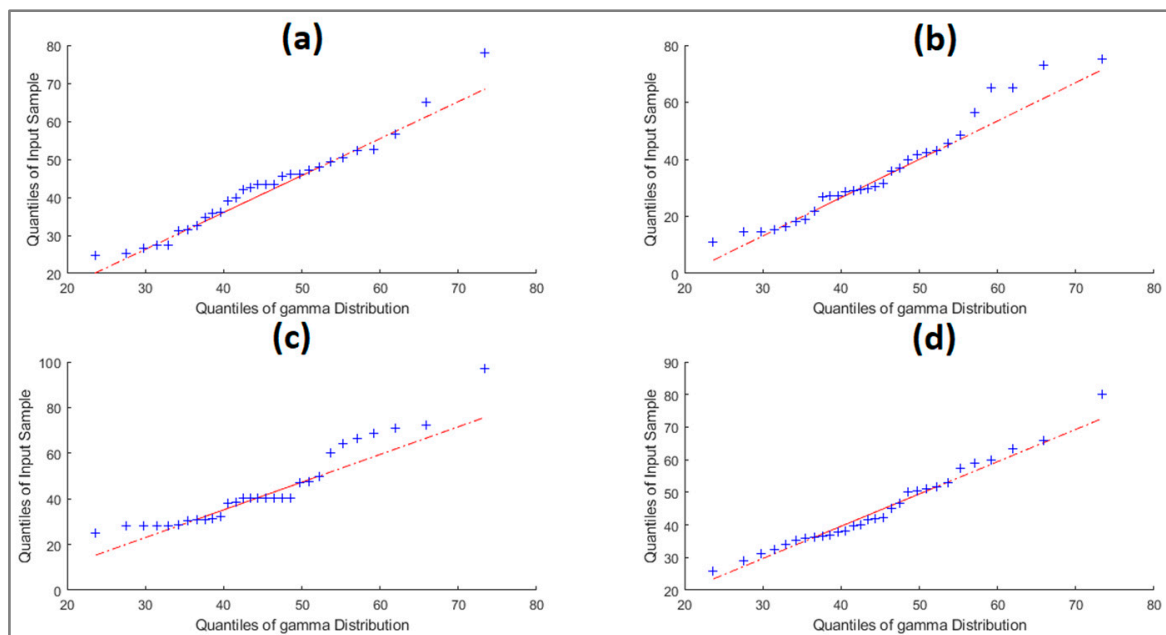


Figure A3. QQ plots gamma distribution for the four stations; (a) 16022, (b) 16247, (c) 16055 and (d) 16081. Blue plus signs are the gamma adjusted precipitation and dotted lines theoretical gamma quantiles.

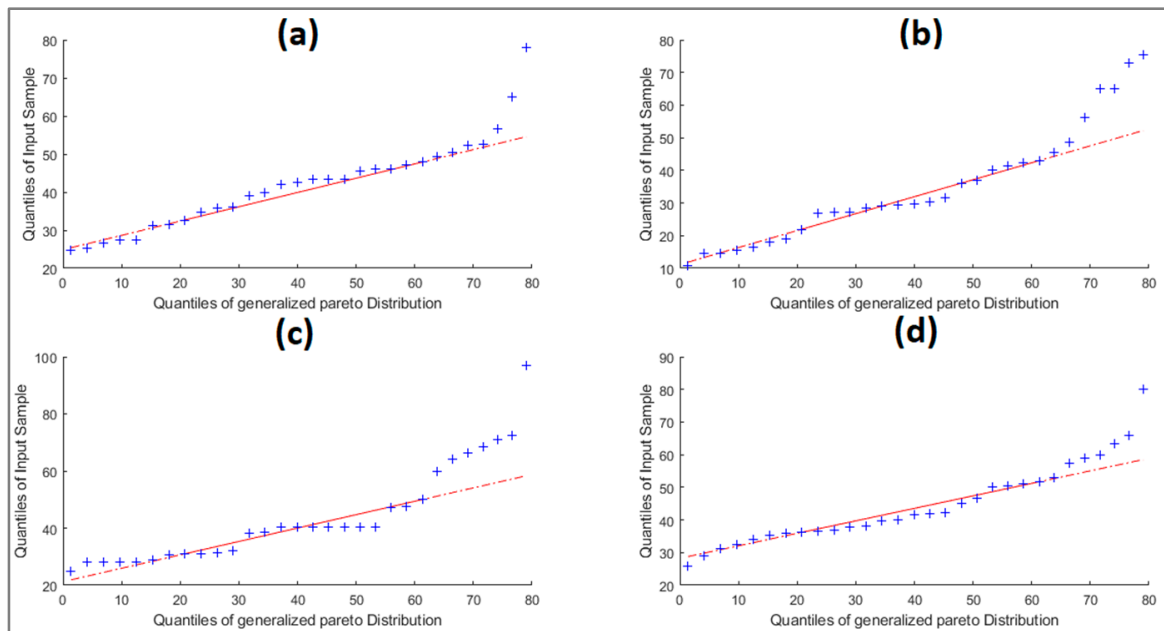


Figure A4. QQ plots generalized pareto distribution for the four stations; (a) 16022, (b) 16247, (c) 16055, and (d) 16081. Blue plus signs are the generalized pareto adjusted precipitation and dotted lines theoretical generalized pareto quartiles.

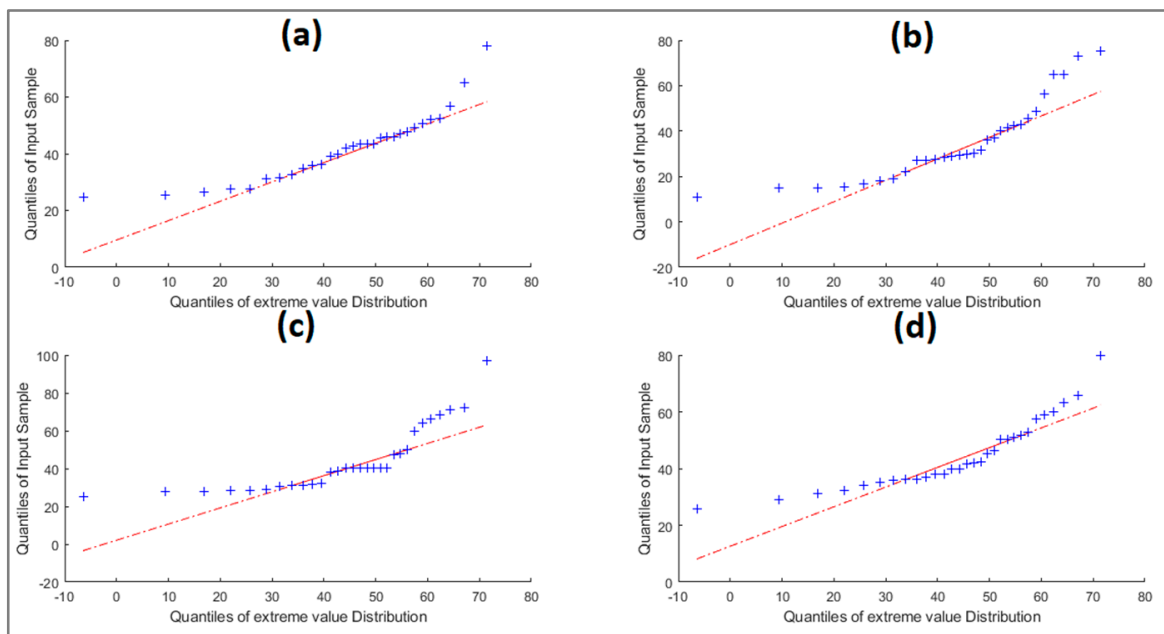


Figure A5. QQ plots Gumbel distribution for the four stations; (a) 16022, (b) 16247, (c) 16055, and (d) 16081. Blue plus signs are the gumbel adjusted precipitation and dotted lines theoretical gumbel quartiles.

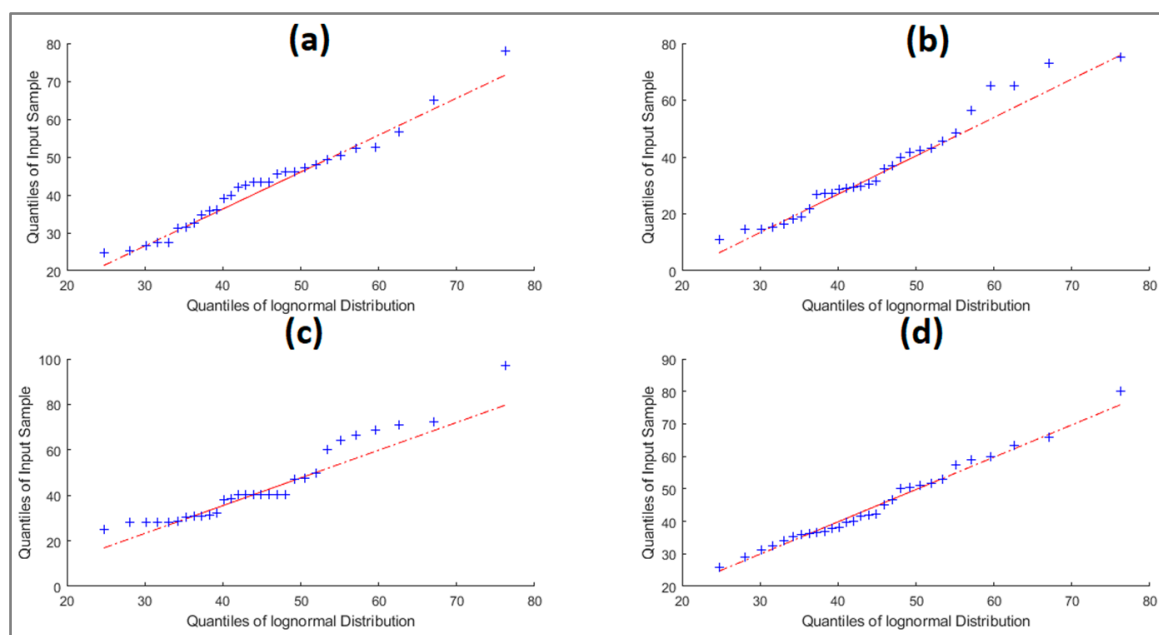


Figure A6. QQ plots log-normal distribution for the four stations; (a) 16022, (b) 16247, (c) 16055, and (d) 16081. Blue plus signs are the log-normal adjusted precipitation and dotted lines theoretical log-normal quantiles.

References

1. Beneyto, C.; Aranda, J.Á.; Benito, G.; Francés, F. New Approach to Estimate Extreme Flooding Using Continuous Synthetic Simulation Supported by Regional Precipitation and Non-Systematic Flood Data. *Water* **2020**, *12*, 3174. [\[CrossRef\]](#)
2. Abreu, M.C.; Cecílio, R.A.; Pruski, F.F.; dos Santos, G.R.; de Almeida, L.T.; Zanetti, S.S. Criteria for Choosing Probability Distributions in Studies of Extreme Precipitation Events. *Rev. Bras. Meteorol.* **2018**, *33*, 601–613. [\[CrossRef\]](#)
3. Segura-Beltrán, F.; Sanchis-Ibor, C.; Morales-Hernández, M.; González-Sanchis, M.; Bussi, G.; Ortiz, E. Using Post-Flood Surveys and Geomorphologic Mapping to Evaluate Hydrological and Hydraulic Models: The Flash Flood of the Girona River (Spain) in 2007. *J. Hydrol.* **2016**, *541*, 310–329. [\[CrossRef\]](#)
4. Kastridis, A.; Theodosiou, G.; Fotiadis, G. Investigation of Flood Management and Mitigation Measures in Ungauged Natura Protected Watersheds. *Hydrology* **2021**, *8*, 170. [\[CrossRef\]](#)
5. Coronado-Hernández, Ó.E.; Merlano-Sabalza, E.; Díaz-Vergara, Z.; Coronado-Hernández, J.R. Selection of Hydrological Probability Distributions for Extreme Rainfall Events in the Regions of Colombia. *Water* **2020**, *12*, 1397. [\[CrossRef\]](#)
6. Flowers-Cano, R.S.; Ortiz-Gómez, R. Comparison of Four Methods to Select the Best Probability Distribution for Frequency Analysis of Annual Maximum Precipitation Using Monte Carlo Simulations. *Theor. Appl. Climatol.* **2021**, *145*, 1177–1192. [\[CrossRef\]](#)
7. Moon, Y.-I.; Lall, U. Kernel Quantite Function Estimator for Flood Frequency Analysis. *Water Resour. Res.* **1994**, *30*, 3095–3103. [\[CrossRef\]](#)
8. Petroselli, A.; De Luca, D.L.; Młyński, D.; Wałęga, A. Modelling Annual Maximum Daily Rainfall with the STORAGE (STOchastic RAInfall GENERator) Model. *Hydrol. Res.* **2022**, *53*, 547–561. [\[CrossRef\]](#)
9. Ciupak, M.; Ozga-Zieliński, B.; Tokarczyk, T.; Adamowski, J. A Probabilistic Model for Maximum Rainfall Frequency Analysis. *Water* **2021**, *13*, 2688. [\[CrossRef\]](#)
10. Tarpanelli, A.; Franchini, M.; Brocca, L.; Camici, S.; Melone, F.; Moramarco, T. A Simple Approach for Stochastic Generation of Spatial Rainfall Patterns. *J. Hydrol.* **2012**, *472–473*, 63–76. [\[CrossRef\]](#)
11. Alodah, A.; Seidou, O. Assessment of Climate Change Impacts on Extreme High and Low Flows: An Improved Bottom-Up Approach. *Water* **2019**, *11*, 1236. [\[CrossRef\]](#)
12. Lele, S.; Keim, J.L. Weighted Distributions and Estimation of Resource Selection Probability Functions. *Ecology* **2006**, *87*, 3021–3028. [\[CrossRef\]](#) [\[PubMed\]](#)
13. Venkata Rao, G.; Venkata Reddy, K.; Srinivasan, R.; Sridhar, V.; Umamahesh, N.V.; Pratap, D. Spatio-Temporal Analysis of Rainfall Extremes in the Flood-Prone Nagavali and Vamsadhara Basins in Eastern India. *Weather Clim. Extrem.* **2020**, *29*, 100265. [\[CrossRef\]](#)
14. Dasallas, L.; An, H.; Lee, S. Developing an Integrated Multiscale Rainfall-Runoff and Inundation Model: Application to an Extreme Rainfall Event in Marikina-Pasig River Basin, Philippines. *J. Hydrol. Reg. Stud.* **2022**, *39*, 100995. [\[CrossRef\]](#)
15. Gabriel, K.R.; Neumann, J. A Markov Chain Model for Daily Rainfall Occurrence at Tel Aviv. *Q. J. R. Meteorol. Soc.* **1962**, *88*, 90–95. [\[CrossRef\]](#)

16. Hernández-Bedolla, J.; Solera, A.; Paredes-Arquiola, J.; Sanchez-Quispe, S.T.; Domínguez-Sánchez, C. A Continuous Multisite Multivariate Generator for Daily Temperature Conditioned by Precipitation Occurrence. *Water* **2022**, *14*, 3494. [[CrossRef](#)]
17. Hayhoe, H.N. Improvements of Stochastic Weather Data Generators for Diverse Climates. *Clim. Res.* **2000**, *14*, 75–87. [[CrossRef](#)]
18. Richardson, C.W.; Wright, D.A.; Nofziger, D.L.; Hornsby, A.G. *WGEN: A Model for Generating Daily Weather Variables*; U.S. Department of Agriculture: Washington, DC, USA, 1984.
19. Marcello, D.; Gianni, B.; Ephrem, H.; Simone, B.; Roberto, C.; Bettina, B. CLIMA: A Weather Generator Framework. In Proceedings of the 18th World IMACS/MODSIM Congress, Cairns, Australia, 13–17 July 2009.
20. Stöckle, C.O.; Nelson, R.; Donatelli, M.; Castellvi, F. ClimGen: A Flexible Weather Generation Program. In Proceedings of the 2nd International Symposium Modelling Cropping Systems, Florence, Italy, 16–18 July 2001; pp. 16–18.
21. Semenov, M.A.; Barrow, E.M. *User's guide: LARS-WG A Stochastic Weather Generator for Use in Climate Impact Studies LARS-WG: Stochastic Weather Generator Contents*; Rothamsted: Harpenden, Hertfordshire, UK, 2002.
22. Chen, J.; Brissette, F.P.; Leconte, R. WeaGETS—A Matlab-Based Daily Scale Weather Generator for Generating Precipitation and Temperature. *Procedia Environ. Sci.* **2012**, *13*, 2222–2235. [[CrossRef](#)]
23. Mehrotra, R.; Li, J.; Westra, S.; Sharma, A. A Programming Tool to Generate Multi-Site Daily Rainfall Using a Two-Stage Semi Parametric Model. *Environ. Model. Softw.* **2015**, *63*, 230–239. [[CrossRef](#)]
24. Carter, T.; Posch, M.; Tuomenvirta, H. *SILMUSCEN and CLIGEN User's Guide: Guidelines for the Construction of Climatic Scenarios and Use of a Stochastic Weather Generator in the Finnish*; Academy of Finland: Helsinki, Finland, 1995.
25. Richardson, C.W. Stochastic Simulation of Daily Precipitation, Temperature, and Solar Radiation. *Water Resour. Res.* **1981**, *17*, 182–190. [[CrossRef](#)]
26. Rayner, D.; Achberger, C.; Chen, D. A Multi-State Weather Generator for Daily Precipitation for the Torne River Basin, Northern Sweden/Western Finland. *Adv. Clim. Change Res.* **2016**, *7*, 70–81. [[CrossRef](#)]
27. Humphrey, G.B.; Gibbs, M.S.; Dandy, G.C.; Maier, H.R. A Hybrid Approach to Monthly Streamflow Forecasting: Integrating Hydrological Model Outputs into a Bayesian Artificial Neural Network. *J. Hydrol.* **2016**, *540*, 623–640. [[CrossRef](#)]
28. Portoghese, I.; Bruno, E.; Guyennon, N.; Iacobellis, V. Stochastic Bias-Correction of Daily Rainfall Scenarios for Hydrological Applications. *Nat. Hazards Earth Syst. Sci.* **2011**, *11*, 2497–2509. [[CrossRef](#)]
29. Wang, L.; Onof, C. Analysis of sub-daily rainfall sequences based upon a semi-deterministic multiplicative cascade method. In Proceedings of the International Workshop on Advances in Statistical Hydrology, Taormina, Italy, 23–25 May 2010; pp. 1–9.
30. Vandenberghe, S.; Verhoest, N.E.C.; Buyse, E.; De Baets, B. A Stochastic Design Rainfall Generator Based on Copulas and Mass Curves. *Hydrol. Earth Syst. Sci.* **2010**, *14*, 2429–2442. [[CrossRef](#)]
31. Katz, R.W.; Parlange, M.B. Generalizations of Chain-Dependent Processes: Application to Hourly Precipitation. *Water Resour. Res.* **1995**, *31*, 1331–1341. [[CrossRef](#)]
32. Koch, E.; Naveau, P. A Frailty-Contagion Model for Multi-Site Hourly Precipitation Driven by Atmospheric Covariates. *Adv. Water Resour.* **2015**, *78*, 145–154. [[CrossRef](#)]
33. Ailliot, P.; Allard, D.; Monbet, V.; Naveau, P. Stochastic Weather Generators: An Overview of Weather Type Models. *J. Société Française Stat. Rev. Stat. Appliquée* **2015**, *156*, 101–113.
34. Wilks, D.S. Multisite Generalization of a Daily Stochastic Precipitation Generation Model. *J. Hydrol.* **1998**, *210*, 178–191. [[CrossRef](#)]
35. Anderson, R.L. Distribution of the Serial Correlation Coefficient. *Ann. Math. Stat.* **1942**, *13*, 1–13. [[CrossRef](#)]
36. Moors, D.S.; Stubblebine, J.B. Chi-Square Tests for multivariate normality with application to common stock prices. *Commun. Stat.-Theory Methods* **1981**, *10*, 713–738.
37. Hu, S. Akaike Information Criterion Statistics. *Math. Comput. Simul.* **1987**, *29*, 452. [[CrossRef](#)]
38. Lima, A.O.; Lyra, G.B.; Abreu, M.C.; Oliveira-Júnior, J.F.; Zeri, M.; Cunha-Zeri, G. Extreme Rainfall Events over Rio de Janeiro State, Brazil: Characterization Using Probability Distribution Functions and Clustering Analysis. *Atmos. Res.* **2021**, *247*, 105221. [[CrossRef](#)]
39. Simolo, C.; Brunetti, M.; Maugeri, M.; Nanni, T. Improving Estimation of Missing Values in Daily Precipitation Series by a Probability Density Function-Preserving Approach. *Int. J. Climatol.* **2010**, *30*. [[CrossRef](#)]
40. Li, C.; Singh, V.P.; Mishra, A.K. Simulation of the Entire Range of Daily Precipitation Using a Hybrid Probability Distribution. *Water Resour. Res.* **2012**, *48*, 3521. [[CrossRef](#)]
41. Shin, Y.; Park, J.S. Modeling Climate Extremes Using the Four-Parameter Kappa Distribution for r-Largest Order Statistics. *Weather Clim. Extrem.* **2023**, *39*, 100533. [[CrossRef](#)]
42. Alahmadi, F.S.; Rahman, N.A. Climate Change Impacts on Extreme Rainfall Frequency Prediction. *J. Water Clim. Change* **2020**, *11*, 935–943. [[CrossRef](#)]
43. Nwaogazie, I.L.; Sam, M.G.; Enciso, R.Z.; Gonsalves, E. Probability and Non-Probability Rainfall Intensity-Duration-Frequency Modeling for Port-Harcourt Metropolis, Nigeria. *Int. J. Hydrol.* **2019**, *3*, 66–75. [[CrossRef](#)]
44. Bajirao, T.S. Comparative Performance of Different Probability Distribution Functions for Maximum Rainfall Estimation at Different Time Scales. *Arab. J. Geosci.* **2021**, *14*, 2138. [[CrossRef](#)]
45. Devkota, S.; Shakya, N.M.; Sudmeier-Rieux, K.; Jaboyedoff, M.; Van Westen, C.J.; Mcadoo, B.G.; Adhikari, A. Development of Monsoonal Rainfall Intensity-Duration-Frequency (IDF) Relationship and Empirical Model for Data-Scarce Situations: The Case of the Central-Western Hills (Panchase Region) of Nepal. *Hydrology* **2018**, *5*, 27. [[CrossRef](#)]

46. Pizarro, R.; Valdés, R.; García-Chevesich, P.; Vallejos, C.; Sangüesa, C.; Morales, C.; Balocchi, F.; Abarza, A.; Fuentes, R. Latitudinal Analysis of Rainfall Intensity and Mean Annual Precipitation in Chile. *Chil. J. Agric. Res.* **2012**, *72*, 252–261. [[CrossRef](#)]
47. Villón-Béjar, M. HidroEsta, Software for Hydrological Calculations. *Rev. Tecnol. En Marcha* **2016**, *29*, 95–108. [[CrossRef](#)]
48. Villón Béjar, M. HidroEsta, Software Para Cálculos Hidrológicos. *Tecnol. En Marcha* **2005**, *18*, 67.
49. Villón Béjar, M. HidroEsta, Software Para Cálculos Hidrológicos y Estadísticos Aplicados a La Hidrología. *Rev. Digit. Matemática Educ. E Internet* **2014**, *12*, 1–8. [[CrossRef](#)]
50. García Castro, E.G. *Estimación de caudales máximos en el río Chira, utilizando métodos estadísticos de Gumbel y de Pearson tipo III*; Universidad Nacional de Piura: Castilla, Piura, Peru, 2023.
51. Mendoza, R.; Zavala, J.; Villa, S. Revisión de Gastos de Diseño de La Presa Huites Mediante Relaciones Lluvia-Escurrimiento. *Ing. Hidráulica Y Ambient.* **2014**, *XXXV*, 77–89.
52. Yu, B. Theoretical Justification of SCS Method for Runoff Estimation. *J. Irrig. Drain. Eng.* **1998**, *124*, 306–310. [[CrossRef](#)]
53. Hawkins, R.H.; Hjelmfelt, A.T.; Zevenbergen, A.W. Runoff Probability, Storm Depth, and Curve Numbers. *J. Irrig. Drain. Eng.* **1985**, *111*, 330–340. [[CrossRef](#)]
54. Yu, B. Validation of SCS Method for Runoff Estimation. *J. Hydrol. Eng.* **2012**, *17*, 1158–1163. [[CrossRef](#)]
55. Boughton, W.C. A Review of the USDA SCS Curve Number Method. *Aust. J. Soil Res.* **1989**, *27*, 511–523. [[CrossRef](#)]
56. Hooshyar, M.; Wang, D. An Analytical Solution of Richards' Equation Providing the Physical Basis of SCS Curve Number Method and Its Proportionality Relationship. *Water Resour. Res.* **2016**, *52*, 6611–6620. [[CrossRef](#)]
57. Kirkby, M.; Cerdà, A. Following the Curve? Reviewing the Physical Basis of the SCS Curve Number Method for Estimating Storm Runoff. *Hydrol. Process.* **2021**, *35*, e14404. [[CrossRef](#)]
58. Stathi, E.; Kastridis, A.; Myronidis, D. Analysis of Hydrometeorological Characteristics and Water Demand in Semi-Arid Mediterranean Catchments under Water Deficit Conditions. *Climate* **2023**, *11*, 137. [[CrossRef](#)]
59. Verma, S.; Verma, R.K.; Mishra, S.K.; Singh, A.; Jayaraj, G.K. A Revisit of NRCS-CN Inspired Models Coupled with RS and GIS for Runoff Estimation. *Hydrol. Sci. J.* **2017**, *62*, 1891–1930. [[CrossRef](#)]
60. Satheeshkumar, S.; Venkateswaran, S.; Kannan, R. Rainfall–Runoff Estimation Using SCS–CN and GIS Approach in the Pappireddipatti Watershed of the Vaniyar Sub Basin, South India. *Model. Earth Syst. Environ.* **2017**, *3*, 24. [[CrossRef](#)]
61. Halwatura, D.; Najim, M.M.M. Application of the HEC-HMS Model for Runoff Simulation in a Tropical Catchment. *Environ. Model. Softw.* **2013**, *46*, 155–162. [[CrossRef](#)]
62. Gimeno, L.; Sorí, R.; Vázquez, M.; Stojanovic, M.; Algarra, I.; Eiras-Barca, J.; Gimeno-Sotelo, L.; Nieto, R. Extreme Precipitation Events. *Wiley Interdiscip. Rev. Water* **2022**, *9*, e1611. [[CrossRef](#)]
63. Chen, X.; Hossain, F. Understanding Future Safety of DAMs in a Changing Climate. *Bull. Am. Meteorol. Soc.* **2019**, *100*, 1395–1404. [[CrossRef](#)]
64. Yin, C.; Wang, J.; Yu, X.; Li, Y.; Yan, D.; Jian, S. Definition of Extreme Rainfall Events and Design of Rainfall Based on the Copula Function. *Water Resour. Manag.* **2022**, *36*, 3759–3778. [[CrossRef](#)]
65. Zhu, B.; Chen, J.; Chen, H. Performance of Multiple Probability Distributions in Generating Daily Precipitation for the Simulation of Hydrological Extremes. *Stoch. Environ. Res. Risk Assess.* **2019**, *33*, 1581–1592. [[CrossRef](#)]
66. Chen, J.; Brissette, F.P.; Zielinski, P.A. Constraining Frequency Distributions with the Probable Maximum Precipitation for the Stochastic Generation of Realistic Extreme Events. *J. Extrem. Events* **2015**, *2*, 1550009. [[CrossRef](#)]
67. Chen, J.; Brissette, F.P.; Chaumont, D.; Braun, M. Performance and Uncertainty Evaluation of Empirical Downscaling Methods in Quantifying the Climate Change Impacts on Hydrology over Two North American River Basins. *J. Hydrol.* **2013**, *479*, 200–214. [[CrossRef](#)]
68. Chen, J.; Brissette, F.P.; Zhang, X.J. Hydrological Modeling Using a Multisite Stochastic Weather Generator. *J. Hydrol. Eng.* **2016**, *21*, 04015060. [[CrossRef](#)]
69. Chen, J.; Brissette, F.P.; Leconte, R. Downscaling of Weather Generator Parameters to Quantify Hydrological Impacts of Climate Change. *Clim. Res.* **2012**, *51*, 185–200. [[CrossRef](#)]
70. Hernández-Bedolla, J. *Análisis de Datos Climáticos Como Predictor Para La Gestión Anticipada de Sequias*. Ph.D. Thesis, Universidad Politecnica de Valencia, Valence, Spain, 2022.
71. Sparks, N.J.; Hardwick, S.R.; Schmid, M.; Toumi, R. IMAGE: A Multivariate Multi-Site Stochastic Weather Generator for European Weather and Climate. *Stoch. Environ. Res. Risk Assess.* **2018**, *32*, 771–784. [[CrossRef](#)]
72. Chen, J.; Brissette, F.P.; Leconte, R. A Daily Stochastic Weather Generator for Preserving Low-Frequency of Climate Variability. *J. Hydrol.* **2010**, *388*, 480–490. [[CrossRef](#)]
73. Gu, L.; Chen, J.; Xu, C.; Kim, J.; Chen, H.; Xia, J.; Zhang, L. The Contribution of Internal Climate Variability to Climate Change Impacts on Droughts. *Sci. Total Environ.* **2019**, *684*, 229–246. [[CrossRef](#)]
74. Li, Z.; Brissette, F.; Chen, J. Finding the Most Appropriate Precipitation Probability Distribution for Stochastic Weather Generation and Hydrological Modelling in Nordic Watersheds. *Hydrol. Process.* **2013**, *27*, 3718–3729. [[CrossRef](#)]
75. Rawat, K.S.; Singh, S.K. Estimation of Surface Runoff from Semi-Arid Ungauged Agricultural Watershed Using SCS-CN Method and Earth Observation Data Sets. *Water Conserv. Sci. Eng.* **2017**, *1*, 233–247. [[CrossRef](#)]
76. Ouaba, M.; Saidi, M.E.; Alam, M.J. Bin Flood Modeling through Remote Sensing Datasets Such as LPRM Soil Moisture and GPM-IMERG Precipitation: A Case Study of Ungauged Basins across Morocco. *Earth Sci. Inform.* **2023**, *16*, 653–674. [[CrossRef](#)]

77. Meresa, H. Modelling of River Flow in Ungauged Catchment Using Remote Sensing Data: Application of the Empirical (SCS-CN), Artificial Neural Network (ANN) and Hydrological Model (HEC-HMS). *Model Earth Syst. Environ.* **2019**, *5*, 257–273. [[CrossRef](#)]
78. Topçuoğlu, M.E.; Karagüzel, R.; Doğan, A. Comparison of the SCS-CN and Hydrograph Separation Method for Runoff Estimation in an Ungauged Basin: The Izmit Basin, Turke. *Int. J. Econ. Environ. Geol.* **2022**, *12*, 22–31. [[CrossRef](#)]
79. Ningaraju, H.J.; Kumar, S.B.G.; Surendra, H.J. Estimation of Runoff Using SCS-CN and GIS Method in Ungauged Watershed: A Case Study of Kharadya Mill Watershed, India. *Int. J. Adv. Eng. Res. Sci.* **2016**, *3*, 36–42.
80. Hashim, H.Q.; Sayl, K.N. Incorporating GIS Technique and SCS-CN Approach for Runoff Estimation in the Ungauged Watershed: A Case Study West Desert of Iraq. *Iraqi J. Civ. Eng.* **2022**, *14*, 1–6. [[CrossRef](#)]
81. Nageswara Rao, K. Analysis of Surface Runoff Potential in Ungauged Basin Using Basin Parameters and SCS-CN Method. *Appl. Water Sci.* **2020**, *10*, 47. [[CrossRef](#)]
82. Jeon, J.H.; Lim, K.J.; Engel, B.A. Regional Calibration of SCS-CN L-THIA Model: Application for Ungauged Basins. *Water* **2014**, *6*, 1339–1359. [[CrossRef](#)]
83. Moid Mohammed, A.; Lakshmi Thatiparthi, V.; Rao Pyla, K.; Maryada, A. Estimation of Surface Runoff in an Ungauged Basin Using SCS-CN Method, A Case Study of Manair River Basin in Telangana, India. *Appl. Ecol. Environ. Sci.* **2020**, *8*, 340–350. [[CrossRef](#)]
84. Faouzi, E.; Arioua, A.; Hssaisoune, M.; Boudhar, A.; Elaloui, A.; Karaoui, I. Sensitivity Analysis of CN Using SCS-CN Approach, Rain Gauges and TRMM Satellite Data Assessment into HEC-HMS Hydrological Model in the Upper Basin of Oum Er Rbia, Morocco. *Model Earth Syst. Environ.* **2022**, *8*, 4707–4729. [[CrossRef](#)]
85. Juma, B.; Olang, L.O.; Hassan, M.A.; Mulligan, J.; Shiundu, P.M. Simulation of Flood Peak Discharges and Volumes for Flood Risk Management in the Ungauged Urban Informal Settlement of Kibera, Kenya. *Phys. Chem. Earth* **2022**, *128*, 103236. [[CrossRef](#)]
86. Bharali, B.; Misra, U.K. Numerical Approach for Channel Flood Routing in an Ungauged Basin: A Case Study in Kulsu River Basin, India. *Water Conserv. Sci. Eng.* **2022**, *7*, 389–404. [[CrossRef](#)]
87. Ouaba, M.; El Khalki, E.M.; Saidi, M.E.; Alam, M.J. Bin Estimation of Flood Discharge in Ungauged Basin Using GPM-IMERG Satellite-Based Precipitation Dataset in a Moroccan Arid Zone. *Earth Syst. Environ.* **2022**, *6*, 541–556. [[CrossRef](#)]
88. Forootan, E. GIS-Based Slope-Adjusted Curve Number Methods for Runoff Estimation. *Environ. Monit. Assess.* **2023**, *195*, 489. [[CrossRef](#)]

Disclaimer/Publisher’s Note: The statements, opinions and data contained in all publications are solely those of the individual author(s) and contributor(s) and not of MDPI and/or the editor(s). MDPI and/or the editor(s) disclaim responsibility for any injury to people or property resulting from any ideas, methods, instructions or products referred to in the content.